Gruen/Kahmen (Editors)

Optical 3-D Measurement Techniques

Applications in inspection, quality control and robotics

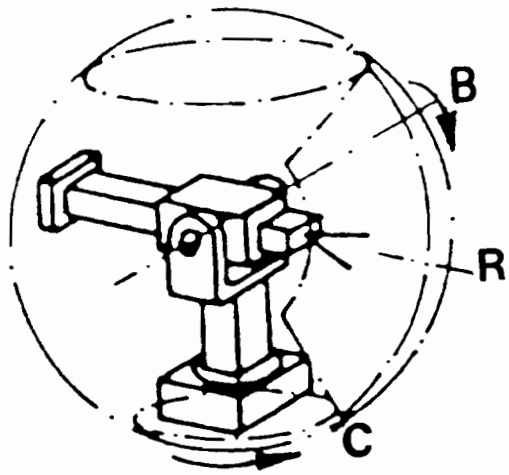

WICHMANN

D. Fritsch

Algorithms in Fast Vision Systems

Abstract

Fast vision systems consist not only of performant hardware; it is especially a chain of algorithms which makes fast vision possible. Therefore main interest has to be directed to an algorithmization allowing different steps in data preprocessing and data analysis.

The paper outlines some methods to be used in digital close range photogrammetry. Two examples demonstrate the efficiency of these methods.

1. Introduction

With the availability of CCD-sensors vision systems could be made possible. These systems allow for automated object tracking, object reconstruction as well as object monitoring to name some tasks especially to solve in machine vision. All these tasks implicate a chain of algorithms ranging from sensor calibration via data preprocessing to data analysis. With regard to real time applications the algorithmisation should be as fast and robust as possible using adequate hardware architecture such as image processors and transputers (A. Grün, 1987).

Although camera calibration remains an object to be investigated furthermore in detail (H.A. Beyer, 1987, R. Lenz / D. Fritsch, 1989) main interest has to be directed to the data flow in data preprocessing and data analysis. This implicates automatically grey value manipulation and grey value evaluation to be reviewed in more detail in the following.

2. Data preprocessing

In order to preprocess the digital image data (digigrams) - for example to compute image gradients or to make the image data more homogeneous - operators should be applied which work as local as possible.

Let the image enhancement or restoration process be written as

$$y(m,n) = \phi\,[x(m,n)] \qquad \forall m = 0,1,2,\ldots,M-1;\ n = 0,1,2,\ldots,N-1 \qquad (1)$$

whereby ϕ characterizes the system or algorithm of the adequate preprocessing. This system may be linear or non-linear (e.g. median filter) depending on the processing step being solved. Although there exist quite a lot of contributions on linear time invariant systems (LTI-systems, L.R. Rabiner / B. Gold, 1975, D. Fritsch, 1982) which allow 'system tuning' in terms of exact approximation, priority should be given to systems working as local as possible. This results into short point spread functions or impulse responses h(m,n) to be used as kernel in the convolution sum

$$y(m,n) = \sum_{k=0}^{K-1} \sum_{l=0}^{L-1} h(k,l)\, x(m-k,n-l) = h(m,n) * x(m,n) \quad (2)$$

Because the impulse response h(m,n) of the system ϕ has to be short (2) is also the implementation rule for data preprocessing. In order to care for zero phased y(m,n) it must be shifted by (K-1)/2, L-1)/2 pixels resulting in

$$y(m,n) = \sum_{k=-(K-1)/2}^{(K-1)/2} \sum_{l=-(L-1)/2}^{(L-1)/2} h(k,l)\, x\,(m-k,n-l) = h(m,n) * x(m,n) \quad (3)$$

One main problem in image preprocessing is the computation of image gradients. These gradients are the skeletons of the objects and may be used in object reconstruction processes. But before to derive the gradient an image smoothing is appropriate to be realized by lowpass filters.

A very simple lowpass filter is the moving average (MA) filter $h(m,n)_{ij} = 1$ - thus its kernel for a 3x3 averaging looks like

$$h(m,n) = 1/9 \begin{vmatrix} 1 & 1 & 1 \\ 1 & 1 & 1 \\ 1 & 1 & 1 \end{vmatrix} \quad (4)$$

Although this filter already contributes a lot to the homogenization process of images, other filters can be designed from known frequency responses (D. Fritsch, 1982, 1984, H.E. Guangping, 1989). In order to consider the aspect of short kernels system tuning algorithms such as linear complementarity algorithms (D. Fritsch, 1985) must <u>not</u> necessarily be applied.

2.1 Edge detection

For fast edge detection some kernels are known from literature (K.R. Castleman, 1979)

- differentiators
- Sobel, Laplace, Roberts or Kirsch

The experience with these operators gives great benefits for 3x3 operators. A comparison between a simple analytical (3x3) differentiator, the heuristic operators Sobel and Laplace, as well as designed 4x4 and 5x5 differentiators (D. Fritsch, 1987) showed that there is a 'break' in gradient information between length 4 and 5. Two of these operators (single differentiator and Sobel) can be seen in Fig. 1

a) simple analytical

$$\begin{vmatrix} 0 & -1/2 & 0 \\ 0 & 0 & 0 \\ 0 & 1/2 & 0 \end{vmatrix} \qquad \begin{vmatrix} 0 & 0 & 0 \\ -1/2 & 0 & 1/2 \\ 0 & 0 & 0 \end{vmatrix}$$

b) Sobel operator

$$\begin{vmatrix} 1 & 2 & 1 \\ 0 & 0 & 0 \\ 1 & -2 & -1 \end{vmatrix} \qquad \begin{vmatrix} 1 & 0 & -1 \\ 2 & 0 & -2 \\ 1 & 0 & -1 \end{vmatrix}$$

Fig. 1: Differentiator templates

With particular regard to the vectorization of gradients a postprocessing of the gradient may be appropriate. This postprocessing should eliminate local point information but should not have much influence on the edge information. Also here experience showed that non-linear filtering techniques (e.g. median filter) can contribute considerably to homogeneous image gradients.

2.2 Line following

Within the process of line following, various algorithms can be used to move along the ridge of a chain of grey-scale peaks and capture all those image elements which represent edges (P. Haberäcker, 1985). A strategy which has already proved itself in the field of digital photogrammetry (D. Fritsch / G. Strunz, 1988, D. Fritsch, 1989a) is a line following algorithm which is purely pixel-oriented - it is called 'line following by windowing'. The principle on which this algorithm works is illustrated in Fig. 2; the procedure it uses is as follows

0. Define a window of size lxl at a point P(m,n)

1. Compare the image elements within the window with a preset threshold value and calculate the centre of gravity

2. Store the image elements or at least the centres of gravity belonging to an edge, then delete all the grey values within the window

3. Move the window towards the centre of gravity

4. Continue with step 1 if there is no gap;
   otherwise go to 0.

In this way, the window can move within the bounds of eight directions.

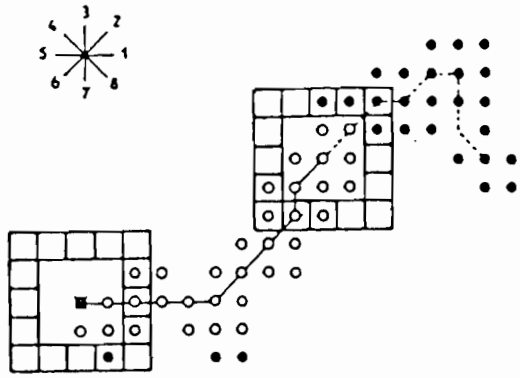

Fig. 2: Line following by windowing

2.3 Vectorization using approximating splines

For vectorization using spline functions, certain continuity requirements can be imposed on the vectorizing function, so that the individual sections of a curve can be joined to one another with no gaps. What will be required is C_0, C_1 or C_2 continuity, depending on whether it is the function values, the first derivations or even the second derivations that are to tally when the curve is joined up.

Since the vectorization of edges generally constitutes a two-dimensional approximation problem, suitable parametrization should also be provided for the spline function applied. One frequently-used form of parametrization uses the arc length t (D. Fritsch, 1989b).

Let

$$z = z(x,y) = \text{const.} \tag{5}$$

be a plane curve in IR^2, further described by the discrete paired values (x_0, y_0), (x_1, y_1), ..., (x_{n-1}, y_{n-1}), representing the position of the image elements. Using the chord sections

$$t_i = \sqrt{(x_i - x_{i-1})^2 + (y_i - y_{i-1})^2} \quad \forall_{i=1,2,3,....,n-1} \tag{6}$$

and

$$t_k = \sum_{i=1}^{k} t_i, \; t_o = 0, \qquad 1 \le k \le n-1 \tag{7}$$

it is possible to approximate arc length t, so that (5) is broken down into

$$z = z(x,y) = \text{const.} \Longrightarrow \begin{cases} x(t) \\ y(t) \end{cases} \quad (8)$$

this being described in discrete form by the paired values (t_o, x_o), (t_o, y_o), (t_1, x_1), (t_1, y_1), ..., (t_{n-1}, x_{n-1}), (t_{n-1}, y_{n-1}).

If every reference point (image element) (t_i, x_i) or (t_i, y_i) is now treated as a node in an approximating spline, then in accordance with (D. Fritsch, 1989b) a spline function g(t) can be formulated, which can satisfy both

$$\int_t (g''(t))^2 \, dt = \min \quad (9)$$

on the one hand, and

$$\sum_{i=o}^{n-1} \left[\frac{g(t_i) - x_i}{\sigma_{xi}} \right]^2 \leq S \quad (10)$$

on the other. The first condition ensures automatic C_2 continuity, while the second condition can control the smoothness of the spline function g(t). This enables adherence to precision specifications σ_{xi} - i.e. admissible deviations between the smoothed function and the original value. To solve equations (9) and (10), the following Lagrangian function is set up and the derivatives of each parameter are obtained:

$$\min_{g(t),\lambda,u} L(g(t),\lambda,u) := \int_{t_o}^{t_{n-1}} (g''(t))^2 \, dt + \lambda \left\{ \sum_{i=o}^{n-1} \left[\frac{g(t_i) - x_i}{\sigma_{xi}} \right]^2 + u^2 - S \right\} \quad (11)$$

This produces a spline

$$s(t) = p_{i,i+1}(t) \quad (12)$$

which is composed of the cubic polynomials

$$p_i(t) = a_i + b_i(t-t_i) + c_i(t-t_i)^2 + d_i(t-t_i)^3 \quad t_i \leq t \leq t_{i+1} \quad (13)$$

For calculation of the coefficients $a_i, b_i, c_i, d_i, \forall i$, please refer to the formulae stated in D. Fritsch (1989b).

To demonstrate the capabilities of this spline approximation, Fig. 3 shows six different degrees of smoothness. In particular, note the variations of the specified precision tolerance σ_r ($=\sigma_{xi}$), which at σ_r = 0.1 (m) reproduces the specified curve with practically no loss of precision, and which at σ_r

= 5.0 (m) reduces it to a straight line. This flexibility can prove to be a considerable advantage in the vectorization of object skeletons, where stretches of gentle curve have to be concatenated with sharply-curved sections and vice versa. On the other hand given that quadrangles and the like are approximated using straight lines only, the spline is useful in offering a wide range of modelling primitives.

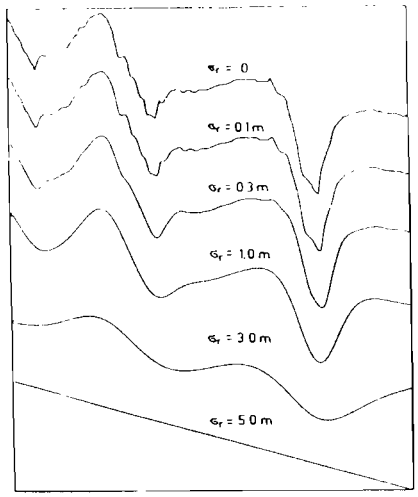

Fig. 3: Variations in smoothness dictated by precision specifications

3. Data analysis

The data analysis in vision systems is consisting of image matching, point determination and object reconstruction or object tracking. The integration of these steps is most recently topic of contributions on digital photogrammetry (B. Wrobel, 1987, H. Ebner et al., 1987, U.A. Helava, 1988). But with regard to vision systems it is more appropriate using fast methods (S.F. El Hakim, 1986, 1989, H. Haggrén, 1986), leading to heuristic procedures which may depend on the problem to be solved. This implicates for image matching not to use image correlation and least squares matching but to apply robust procedures to detect target locations and to solve target matching.

3.1 Target location

The methods for fast target location mostly depend on the target pattern. When using circular targets two main strategies lead to the centre of targets

- estimation of the center of gravity
- computation of best-fit ellipses within the original image or in the image gradient

But before the centre of targets can be computed the targets must be located automatically. For that reason some operators can be used to search for a target pattern represented by a

grey scale mountain and valley respectively. For the examples below we used the moving average filter as location operator because it is capable to reduce the noise level on the targets if any. The final centreing may be supported by a recursion algorithm using a window of kxk pixel, in which for each recursion l=1,2,..., L the centre is computed. This value has to be compared with the proceeding centre; if

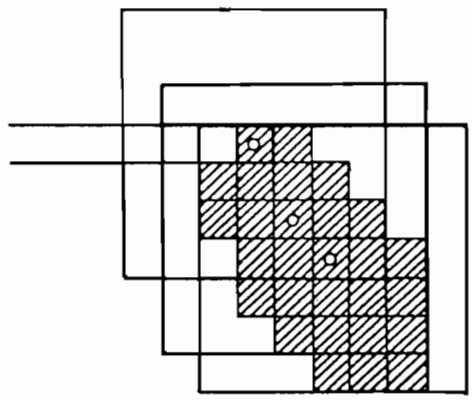

Fig. 4: Window centreing

$$m_L,\ n_L \ - \ m_{L-1},\ n_{L-1} \ \leq 1 \text{ pixel} \qquad (14)$$

the optimum centre is found (see Fig. 4).

In some cases the centre calculation is not satisfactory because changes of imaging conditions cause variable results. It is more reliable to compute real ellipse centres (G. Zhou, 1986).

Let be

$$a(x_i-x_o)^2 + 2b(x_i-x_o)(y_i-y_0 + c(y_i-y_o)^2 = 1 \quad i=1,2,... \qquad (15)$$

the constraint equation for an ellipse in which x_i, y_i represents the pixel location at the corner of the ellipse. Then the parameters a, b, c as well as the exact centre x_o, y_o can be obtained by a least-squares fit using the centre coordinates as approximate values. Another strategy for the derivation of ellipse centres is to find two diameters and then to calculate this intersection which is the centre of the ellipse. In Fig. 5 ellipse centreing by means of least-squares fits can be found - the experience showed that the exact centres can be estimated with an accuracy of about

$$1/20 \leq \sigma_{x,y} \leq 1/10 \text{ pixel size} \tag{16}$$

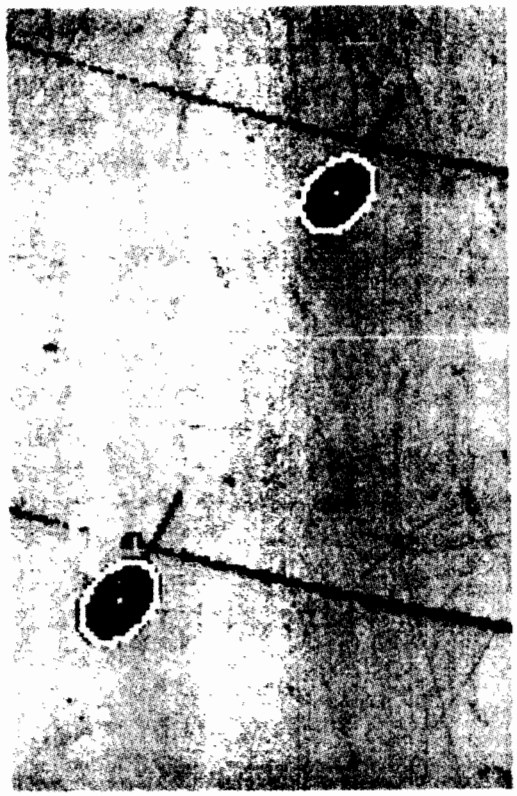

Fig. 5: Best-fit ellipses of targets

3.2 Target matching

The target matching problem can be solved using the collinearity equations or the coplanarity condition. Each point in one image (master) has to be matched with its corresponding point taken by another camera (slave image). When using known exterior orientation parameters the result is a straight line (epipolar line)

$$y_2 = ax_2 + b \tag{17}$$

in which the parameters a and b are given by the image perspectives. All coordinates of the slave image can be introduced into (17) and must be compared with a threshold T. If

$$\Delta = ax_2 + b - y_2 \leq T \tag{18}$$

the points match each other. Occasionally more than one target will satisfy (18) therefore the strategy may be reversed to match a point in the slave image with its corresponding point in the master image.

3.3 Combined point determination and object reconstruction

If the image coordinates of the targets or other points are known the coordinates of object space can be derived by bundle block adjustment or simply by using the collinearity equations in case of two images. As far as simple objects are concerned, there is often object (prior) information available to be considered within the point determination process. Therefore the point determination has to introduce all informations on the object itself leading to combined point determination. Especially in machine vision applications information on the shape or surface of the object is often given. This can be in form of analytical descriptions (e.q. cube, paraboloid) or by digital surface models in case of more complex structures.

4. Examples

For demonstration of the algorithms proposed in this paper two examples will be treated

- reconstruct a cube of 20 (cm) side length by means of three synthetic images
- reconstruct a subreflector by means of three scanned analogous WILD P31 photographs

The first example served as 'study object' to check the algorithmization whereas the second one was a real benchmark with regard to robustness and modelling primitives.

4.1 Reconstruction of a cube

To reconstruct a cube of 20 (cm) side length three synthetic digital images were generated considering a CCD-sensor of 245 H x 319 V pixels. The size of the digital image was supposed to be 6.6 x 8.6 (mm) leading to a pixel size of about 0.027 (mm). The location of the three synthetic CCD cameras can be seen in Fig. 6

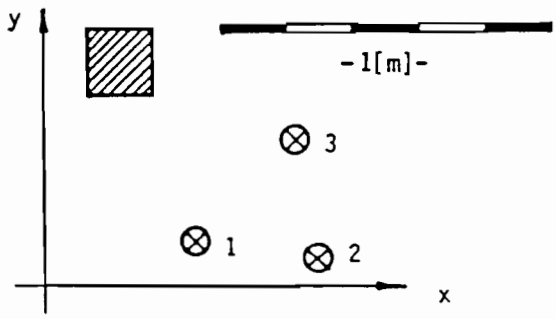

Fig. 6: Location of the CCD cameras

For the reconstruction of the cube two strategies are compared with each other: the first one using image coordinates of the targets and the second one using the image coordinates of corners of the cube. The reconstruction of the cube makes use of the condition equations

$$\left\{(X_k-X_i)^2 + (Y_k-Y_i)^2 + (Z_k-Z_i)^2\right\}^{\frac{1}{2}} =: |\overrightarrow{P_iP_k}| = a \qquad (19a)$$

$$\alpha = \cos^{-1}\left\{\frac{(\overrightarrow{P_iP_j})(\overrightarrow{P_iP_k})}{(\overrightarrow{P_iP_j})(\overrightarrow{P_iP_j})}\right\} = \pi/2 \qquad (19b)$$

which have been considered partly within the bundle block adjustment (eq. 19b). This implicates a chain of algorithms given by Table 1 in which the original images (Fig. 7a) and the image gradients (Fig. 7a-c) are used.

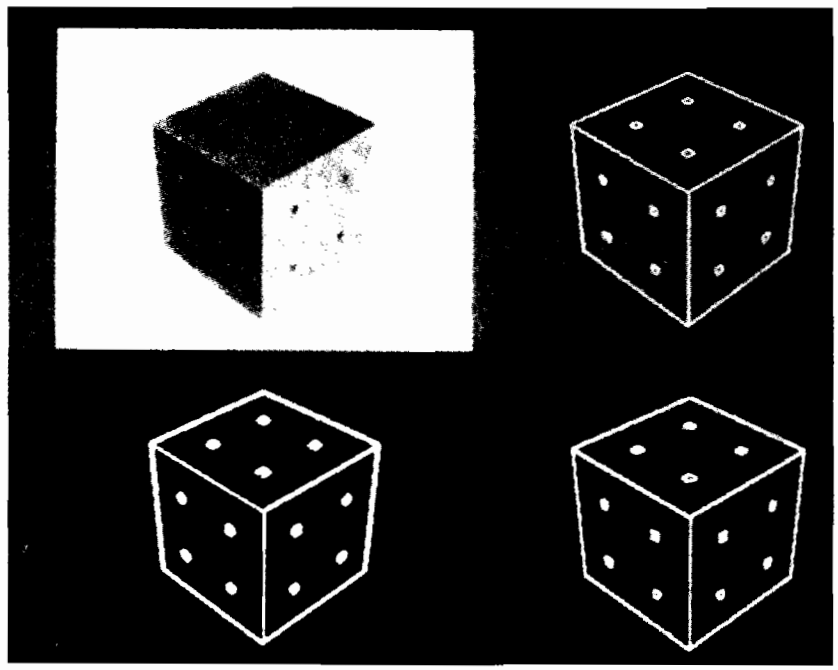

Fig. 7: Image 2 of the cube and its corresponding gradients
a) original image (b) gradient of simple differentiator
c) gradient of Sobel (d) gradient of 5x5 differentiator

Table 1: Algorithms to reconstruct the cube

step	original images	image gradients
1	target location by means of the MA-operator	vectorization by means of line following and best-fit straight lines
2	computation of image coordinates (centres of gravity and best-fit ellipses)	computation of image coordinates of the corners of the cube
3	image matching using the master and its slaves	image matching using the master and its slaves
4	point determination by bundle block adjustment	point determination by bundle block adjustment
5	best-fit planes, intersection of straight lines and reconstruction of the cube	reconstruction of a best-fit cube

The cube was reconstructed under the premise of different signal/noise ratios (SNR); its side length and corresponding standard deviation can be found in Table 2

Table 2: Reconstruction of the cube

SNR	original images		image gradient	
	a	σ_a	a	σ_a
0	19.989	0.023	20.128	0.027
1	19.990	0.030	20.131	0.029
5	19.991	0.043	20.132	0.032
10	19.977	0.054	20.136	0.036

A comparison of the results gives clear advantages for the use of target information in the original images, because the geometry in machine vision applications is mostly poor. But when using more than three CCD cameras optimization strategies and here especially first order design to fix the camera positions is highly recommended. The estimation of the accuracy of image coordinates a posteriori amounts to $\sigma=5.5\text{x}10^{-4}$ (cm) and corresponds to about 20% of the pixel size.

4.2 Reconstruction of a subreflector

For the reconstruction of a subreflector three analogous images of a WILD P31 camera with c=103.34 (mm) habe been scanned with a Hell scanner Chromagraph CTX 330 with a resolution of 0.01 (mm). This led to three digigrams of 120 MB for each; one digital image can be seen in Fig. 8.

(a) (b)

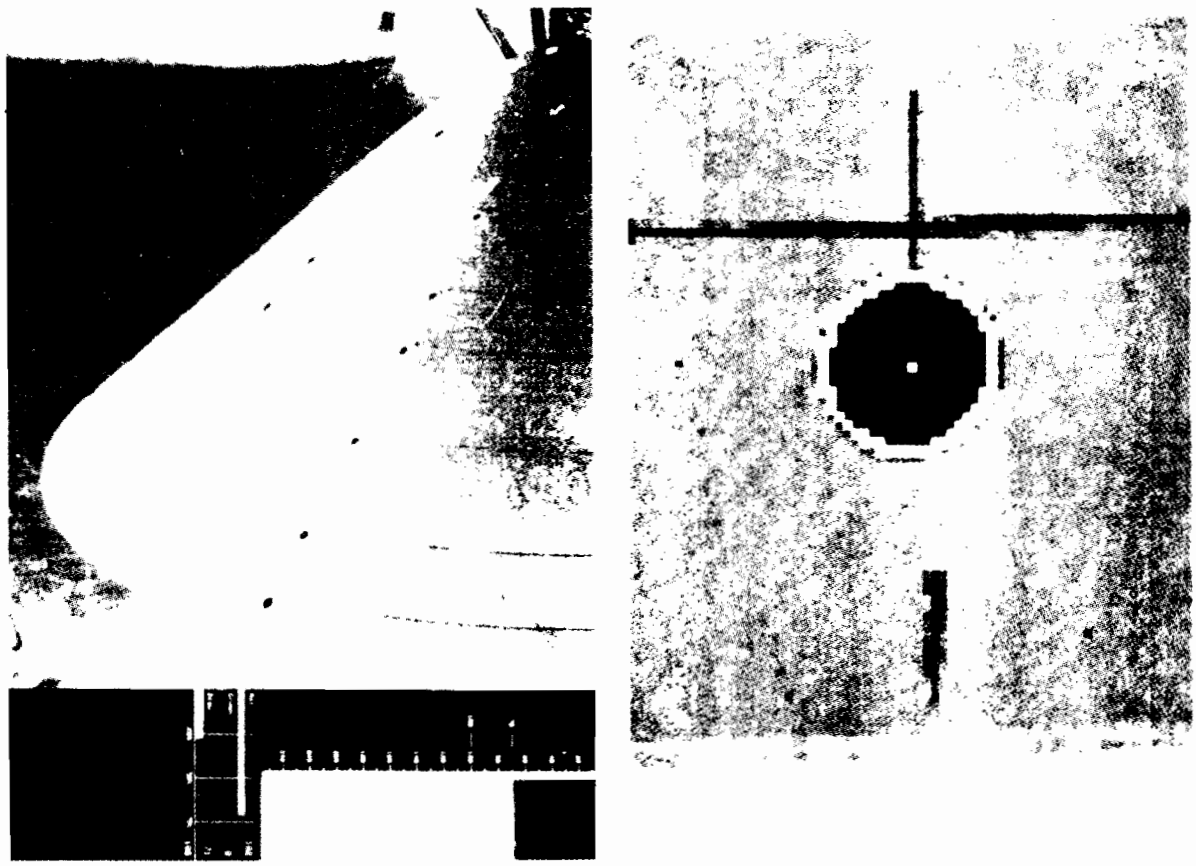

Fig. 8: Digital image of the subreflector
a) global view b) detailled view

The targets used in the data analysis were twofold: on the one hand circular targets could be identified consisting of labels which number the intersection of meridians and parallel circles (see Fig. b) and on the other hand these intersections itself were the targets. The algorithmization used for the point determination is given by Table 3.

Table 3: Algorithmus for 3D point determination

step	algorithm
0	identification of fiducial marks by means of best-fit straight lines and its intersections
1	determination of the image centre
2	target location by means of the MA-operator
3a	computation of image coordinates of circular targets using the centre of gravity and best-fit ellipses
3b	computation of image coordinates of the intersections of meridians and parallel circles by means of best-fit straight lines and lower order least-squares polynomials
4	image matching using the master and its slaves
5	point determination by bundle block adjustment

For the reconstruction of the subreflector a rotary paraboloid have been used to describe the 3D-point manifold analytically.

With

$$y^2 = 2px = 4fz \tag{20}$$

as formula of a parabel of focus distance p/2=f, that is f is the distance from the vertex origin, a surface depending on $R^2 = x^2 + y^2$ is to describe by

$$R^2 = 4fz \tag{21}$$

This is the formula of a paraboloid with its vertex fixed in the coordinate origin. But (21) cannot be fulfilled in machine vision applications therefore it must be generalised into

$$z = z_o - (x-x_o)\tan B + (y-y_o)\tan A + \frac{R^2}{4f} \tag{22}$$

that is the paraboloid has six datum parameters x_o, y_o, z_o (translations of the vertex), A, B (rotations of the vertex) as well as its focus distance f to be interpreted as the scale of the paraboloid. These parameters must be determined in the object reconstruction process. Using the least-squares method a corresponding condition equation to (22) looks like

$$z_i+v_{zi}+k=z_o-(x_i+v_{xi}-x_o)\tan B+(y_i+v_{yi}-y_o)\tan A+ \\ +\frac{(x_i+v_{xi}-x_o)^2+(y_i+v_{yi}-y_o)^2}{4f} \qquad (23)$$

in which k is a constant value to overcome shaped paraboloids. This equation can be treated in correspondance with D. Fritsch et al. 1989 leading to a Gauβ-Markoff model

$$\boxed{E(l) = l + v = Ax\ ,\quad D(l) = \sigma^2 P^{-1}} \qquad (24)$$

which characterises the least-squares descriptions.

The reconstruction of the cube on the basis of a rotary paraboloid led to the parameters given in Table 4

Table 4: Reconstruction of the subreflector

parameter	values
x_o	8317.826 (mm)
y_o	7155.638 (mm)
z_o	537.826 (mm)
A	-0.000757 (rad)
B	-0.000326 (rad)
f	514.964 (mm)
σ	0.121 (mm)

Main interest in such applications is directed to the goodness-of-fit of the surface that is the perpendicular deviation between the theoretical contour and the real contour (see Fig. 9).

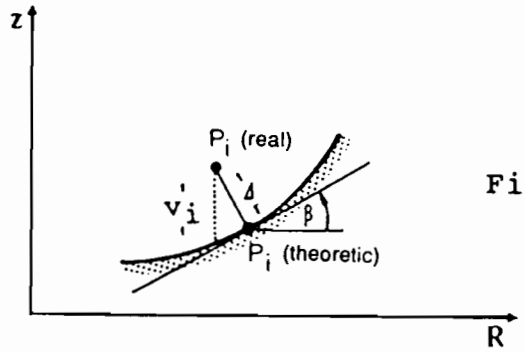

Fig. 9: Projection of the deviation

An estimation of an overall measure defined by RMS = $\sqrt{||\cos\beta v||^2}$ led to RMS = 0.114 (mm). In this way the subreflector is totally described.

5. Conclusions

The experience with the algorithms proposed in the paper gives optimism to realize fast vision system. Although some algorithmic steps are depending on the special application there is a basis software to be used in most applications. In this context can be seen image preprocessing techniques such as edge detection, line following and vectorization as well as image analysis techniques consisting of image matching and point determination. The main point in realization of algorithmic chains should be directed to robustness and speed in order to be competitive with non-vision systems. Even if vision systems have some disadvantages for example illumination conditions and sensor depending errors they should be hardly tested in a lot of pilot applications.

6. Acknowledgements

The author gratefully acknowledges the work carried out by P. Lohse, K. de Laporte and R. Winhart who managed the examples presented in this paper.

References

BEYER, H.A. (1987): Some Aspects of the Geometric Calibration of CCD-Cameras. Proceed. ISPRS Intercomm. Conf. Fast Process. Photogr. Data, Interlaken, Inst. Geod., Photogr. ETH Zürich, pp. 142-155, Zürich.

CASTLEMAN, K.R. (1989): Digital Image Processing. Prentice Hall, Englewood Cliffs, New Jersey.

EBNER, H. / D. FRITSCH / W. GILLESSEN / Ch. HEIPKE (1987): Integration von Bildzuordnung und Objektrekonstruktion innerhalb der Digitalen Photogrammetrie. Bildmess., Luftbildwes. (BuL), 55, S. 194-203.

EL-HAKIM, S.F. (1986): Real-Time Image Metrology with CCD Cameras. Phot. Eng. Rem. Sens., 52, pp. 1757-1766.

EL-HAKIM, S.F. (1989): A Hierarchical Approach to Stereo Vision. Phot. Eng. Rem. Sens., 55, pp. 443-448.

FRITSCH, D. (1982): Entwurf digitaler zweidimensionaler nichtrekursiver Filter. Deutsche Geod.Komm., Reihe C, Nr.275

FRITSCH, D. (1984): Two-Dimensional Finite Impulse Response (FIR) Linear Systems in Digital Photogrammetry. Int. Arch. Phot. Rem. Sens., 25, A3a, pp. 290-300, Rio de Janeiro.

FRITSCH, D. (1985): Some Additional Informations on the Capacity of the Linear Complementarity Algorithm. In: Optimization and Design of Geodetic Networks, Ed. E.W. Grafarend / F. Sanso, Springer, Heidelberg, pp. 169-184.

FRITSCH, D. (1987): On Algorithms Solving the L_∞-Approximation in Geometric Modelling. Proceed. ISPRS Intercomm. Conf. Fast Process. Photogr. Data, Interlaken, Inst. Geod., Photogr., ETH Zürich, pp. 142-155, Zürich

FRITSCH, D. / G. STRUNZ (1988): Towards an Automated Data Flow in Digital Close Range Photogrammetry. Int. Arch. Phot. Rem. Sens., 27, B11, pp. V415-V427, Kyoto.

FRITSCH, D. / H. KLENNERT / R. REISER (1989): Development and Application of an Antenna Measurement and Evaluation System. Allgem. Verm. Nachr. - Int. Edition - , 6, pp. 3-12.

FRITSCH, D. (1989a): On Raster to Vector Conversion in Hybrid Graphic Systems. Proceed. AM/FM Int. Conf., Montreux.

FRITSCH, D. (1989b): Digitale Geländemodelle und Raumbezogene Informationssysteme. Habilitationsschrift Techn. Univ. München (in preparation).

GRÜN, A. (1987): Towards Real-Time Photogrammetry. Photogrammetria, 42, pp. 209-245.

GUANGPING, H.E. (1989): Bildverbesserung mittels digitaler Filterung. Geowiss. Mitt., Heft 31, Techn. Univ. Wien.

HABERÄCKER, P. (1985): Digitale Bildverarbeitung. Hanser, München.

HAGGREN, H. (1986): MAPVISION: The Photogrammetric Machine Vision System for Engineering Applications. Pres. Paper, SPIE's Symp. Optic., Optoelectr. Engin., Cambridge.

HELAVA , U. (1988): Object Space Least Squares Correlation. Int. Arch. Phot. Rem. Sens., 27, B3, pp. 321-331, Kyoto.

LENZ, R. / D. FRITSCH (1989): On the Accuracy of Videometry with CCD-Sensors. Photogrammetria, 44 (in print).

LOHSE, P. / K. de LAPORTE (1988): Zur automatischen Erfassung von Bilddaten in digitalen Meßbildern. Diplomarbeit Techn. Univ. München (not published).

RABINER, L.R. / B. GOLD (1975): Theory and Application of Digital Signal Processing. Prentice Hall, Englewood Clifts.

WINHART, R. (1989): Rekonstruktion eines Subreflektors vermittels digitaler Photogrammetrie. Diplomarbeit Techn. Univ. München (not published).

WROBEL, B. (1987): Facets Stereo Vision (FAST Vision) - A New Approach to Computer Stereo Vision and to Digital Photogrammetry. Proceed. ISPRS Intercomm. Conf. Fast Process. Photogr. Data, Interlaken, Inst. Geod., Photogr., ETH Zürich, pp. 231-258, Zürich.

ZHOU, G. (1986): Accurate Determination of Ellipse Centres in Digital Imagery. Proceed. 1986 ACSM-ASPRS Ann. Conv., 4, pp.